energies

MDPI

Article

Determination of the Radiation Exchange Factor in the Bundle of Steel Round Bars

Rafał Wyczółkowski [1,*], Marek Gała [2], Stanisław Szwaja [3] and Andrzej Piotrowski [4]

[1] Department of Production Management, Czestochowa University of Technology, Armii Krajowej 19, 42-200 Czestochowa, Poland
[2] Institute of Electric Power Engineering, Czestochowa University of Technology, Armii Krajowej 17, 42-200 Czestochowa, Poland; marek.gala@pcz.pl
[3] Department of Thermal Machinery, Czestochowa University of Technology, Armii Krajowej 21, 42-200 Czestochowa, Poland; szwaja@imc.pcz.czest.pl
[4] Department of Technology and Automation, Czestochowa University of Technology, Armii Krajowej 21, 42-200 Czestochowa, Poland; andrzej.piotrowski@pcz.pl
* Correspondence: rafal.wyczolkowski@pcz.pl

Abstract: A method to obtain a radiation exchange factor F_R in the bundle of steel round bars is presented. This parameter is required for determination of the radiative thermal conductivity k_{rd}, which is one of the basic thermal properties of the bar bundles. In the presented approach, the analyzed parameter is calculated indirectly. The initial point for calculations is the geometric model of the medium defined as a unit cell. Then, for the elements present in this cell, the thermal resistance of both conduction and radiation is determined. The radiation resistance is calculated from the radiosity balance of the surfaces enclosing the analyzed system. On this basis, the radiation thermal conductivity k_{rd} is calculated. Next, taking into account the bar diameter, the value of parameter F_R is also determined. The analysis is performed at the process temperature range of 200 to 800 °C for three bar diameters: 10, 20 and 30 mm, and for the three porosities of the bundle. Different emissivity of bars in the range of 0.5 to 0.9 was also taken into account. Finally, a relationship that allows calculating the F_R factor correlated with the emissivity of the bars and the bundle porosity was established. The k_{rd} obtained from the methodology presented and compared with the values calculated directly do not exceed 9%; however, after averaging over the entire temperature range of the process, the difference does not exceed 0.2%.

Keywords: bar bundle; heat treatment; thermal radiation; radiation thermal conductivity; radiation exchange factor; effective thermal conductivity

Citation: Wyczółkowski, R.; Gała, M.; Szwaja, S.; Piotrowski, A. Determination of the Radiation Exchange Factor in the Bundle of Steel Round Bars. *Energies* **2021**, *14*, 5263. https://doi.org/10.3390/en14175263

Academic Editors: Heping Tan and Kang Luo

Received: 26 June 2021
Accepted: 21 August 2021
Published: 25 August 2021

1. Introduction

Steel bars are the primary metallurgical components that are widely used in various fields of the industrial manufacturing. Similar to most steel products, these steel bars are manufactured by a rolling process. Such metalworking usually does not provide the required mechanical and technological properties of the final product. Therefore, the bars require additional heat treatment [1]. Heat treatment operations have a significant impact on energy consumption, production efficiency, and pollutants emissions to the natural environment, and obviously they have an impact on the quality of the final product. Hence, the heat treatment process has to be optimized. This is often performed by computational analysis of the appropriate numerical models [2–4]. The thermal properties of a heated element are important parameters for these analytical models.

To ensure the most efficient use of a furnace chamber, the treated bars are usually heated in the form of cylindrical bundles. As shown in Figure 1, the bundle of round bars has a porous structure, which makes the effective thermal conductivity k_{ef} its basic thermal property [5]. Contrary to the thermal conductivity of homogeneous substances, this parameter is not a material property.

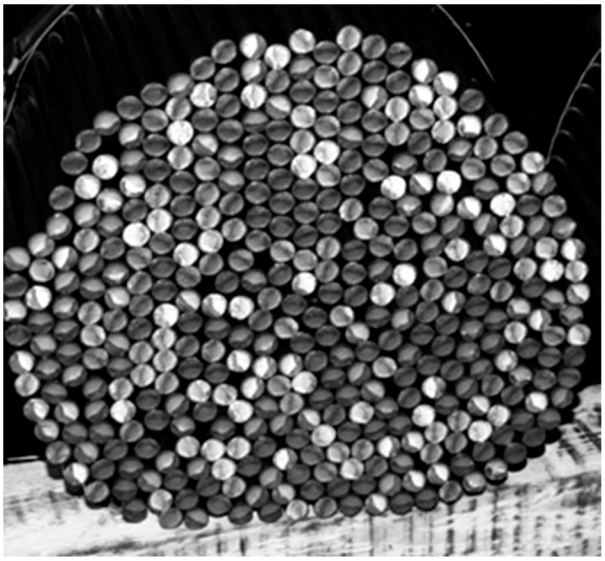

Figure 1. Example of the round bar bundle showing its cell-based structure.

The effective thermal conductivity of the bar bundle is a function of the complex heat transfer mechanisms related to conduction and radiation and can be defined as the sum of two components, the essential thermal conductivity k_{es} and the radiation thermal conductivity k_{rd} (Equation (1)) [6,7]:

$$k_{ef} = k_{es} + k_{rd}, \quad (1)$$

The coefficient k_{es} represents the heat transferred by conduction in the bundle, while k_{rd} relates to the heat transferred by radiation. Thus, one of the thermal properties of the bar bundle is k_{rd} and its value can be determined analytically. Most often the concept of a unit cell is used for this purpose. This approach uses periodically repeated elements of idealized geometry. In spherical or cylindrical particle systems, the k_{rd} is generally calculated as the quotient of the radiation exchange factor F_R, the Stefan–Boltzmann constant σ, particle diameter d_p, and the third power of the mean absolute temperature of the medium T (Equation (2)) [8,9]:

$$k_{rd} = 4F_R\sigma d_p T^3, \quad (2)$$

Despite the simple form of the Equation (2), this approach has a serious limitation, which arises from the difficulties in determining F_R. This factor cannot be easily calculated, which leads to significant discrepancies in the results obtained by researchers [10–13]. There are several correlations that have been developed for packed bed structures. However, these correlations are not suitable for a packed bed of bars as they are developed for materials consisting of spherical particles. In contrast, in the bed of bars, individual elements (particles) have a cylindrical shape. As a result, the geometry of the surfaces closing the space of radiation heat transfer is different in both cases, which results from various values of view factors. The possibility of using various correlations from literature reports for determining the F_R factor for modeling radiation heat transfer in the packed beds of steel bars was analyzed in [14]. Five different computational models were analyzed in detail: Cheng and Churchill [10], Vortmeyer [11], Wakao and Wato [12], Argo and Smith [13], and Kasparek and Vortmeyer [15]. As a result of the calculations, it was shown that these five models gave significantly different F_R in the range from 0.5 to 1.05, while for the bed of steel bars, the F_R was in the range from 0.4 to 0.6. On the basis of these calculations, it was found that the models from studies reported in the literature do not give correct results when the analyzed medium is the bundle of bars. This paper presents an innovative method of determining the F_R radiation exchange factor in the bundle of steel round bars.

2. Materials and Methods

In the proposed approach, the radiation exchange factor F_R for the bundle of steel round bars is calculated from Equation (3), which results from the rearranging Equations (1) and (2):

$$F_R = \frac{k_{rd}}{4\sigma T^3} = \frac{k_{ef} - k_{es}}{4\sigma T^3}, \tag{3}$$

The k_{ef} and k_{es} coefficients, which are required to calculate the F_R factor, were initially determined on the basis of the analysis of thermal resistances. This method is based on the analogy of the phenomena of electrical and thermal conduction, which arise from the similar mathematical notation of two laws: Ohm and Fourier [16]. At the first stage of calculations, a geometric model of the medium considered was developed and analyzed. It was assumed that the medium can be reduced to a flat bed of bars with a staggered arrangement. The repeatable rectangular part of this model is shown in Figure 2a. Based on this geometrical part, equations for the vertical heat flow described by the heat flux vector q (Figure 2b) were worked out.

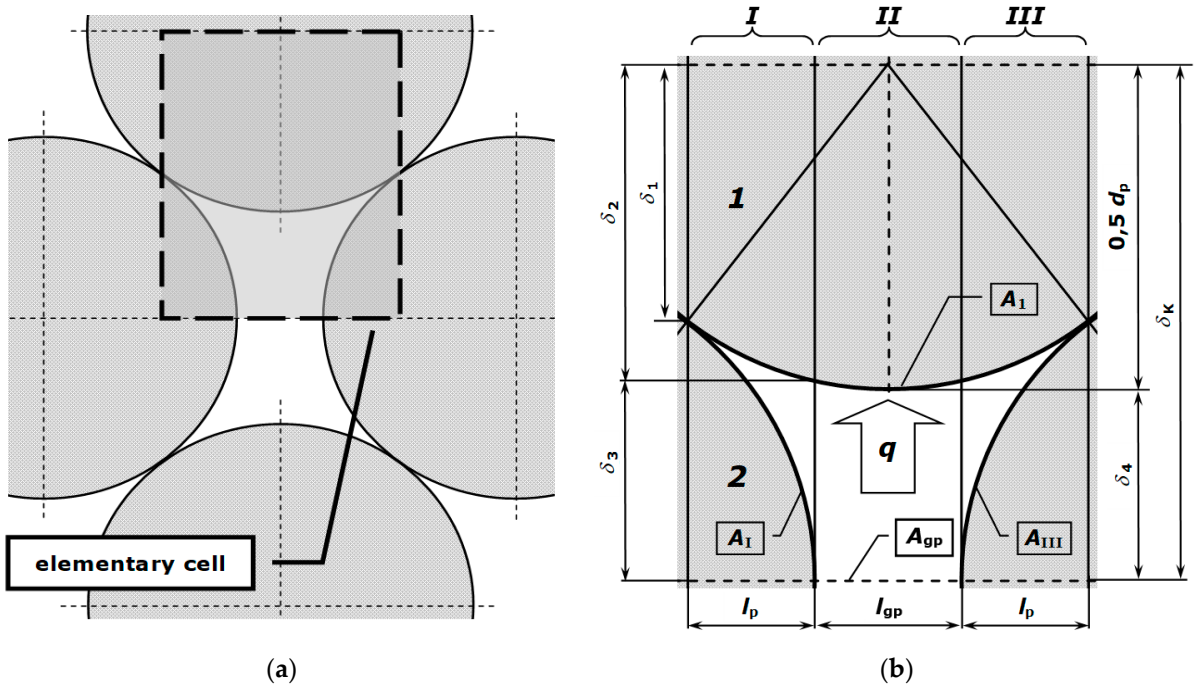

(**a**) (**b**)

Figure 2. (**a**) Part of the considered charge and (**b**) elementary cell used for thermal resistance analysis.

The cell includes fragments of two layers of bars (top layer *1* and bottom layer *2*) and is divided into three sections following sections that are parallel to the vector q: a central section (*II*) and two side sections (*I, III*), which are identical to each other. To define the cell geometry, the bar diameter d_p and the width of the gap between the bars from layer l_{gp} are applied. Based on these two parameters, the cell height δ_K (Equation (4)) and width of the side sections l_p (Equation (5)) are defined:

$$\delta_K = \sqrt{d_p^2 - \left[0.5\left(d_p + l_{gp}\right)\right]^2}, \tag{4}$$

$$l_p = 0.25\left(d_p - l_{gp}\right) \tag{5}$$

The next step of the analysis is the identification of all heat transfer mechanisms occurring within the cell. The heat transfer through the bundle of bars can be modeled as a combined effect of the following mechanisms: (i) conduction through individual bars, (ii) conduction in gas-filled voids, (iii) contact conduction between adjacent bars, and (iv)

thermal radiation between the surfaces of the bars. Each of these mechanisms can be quantified by an appropriate thermal resistance. Referring this problem to the investigated cell, the resistances in the side sections can be distinguished as follows: $R_{\mathrm{I}\,2\mathrm{s}}$ and $R_{\mathrm{III}\,2\mathrm{s}}$ for the conduction in the bars from the bottom layer, $R_{\mathrm{I}\,2\mathrm{g}}$ and $R_{\mathrm{III}\,2\mathrm{g}}$ for the conduction in gas cavity, R_{ct} for contact conduction between adjacent bars, $R_{\mathrm{I\,rd}}$ and $R_{\mathrm{III\,rd}}$ for thermal radiation, and $R_{\mathrm{I}\,1\mathrm{s}}$ and $R_{\mathrm{III}\,2\mathrm{s}}$ for the conduction in the parts of bar from the top layer. In turn, one can distinguish the following resistances for the central section: $R_{\mathrm{II\,g}}$ for the conduction in gas cavity, $R_{\mathrm{II\,rd}}$ for the thermal radiation, and $R_{\mathrm{II}\,1\mathrm{s}}$ for the conduction in the fragment of the bar at the top layer. The total, thermal resistance of the elementary cell R_{to} is calculated as the resultant resistance of the series- and parallel-connected resistances noted above (Equation (6)). The equivalent system of these resistances is shown in Figure 3.

$$R_{\mathrm{to}} = \left[\left(R_{\mathrm{I}\,2\mathrm{s}} + R_{\mathrm{I}} + R_{\mathrm{I}\,1\mathrm{s}} \right)^{-1} + \left(R_{\mathrm{II}} + R_{\mathrm{II}\,1\mathrm{s}} \right)^{-1} + \left(R_{\mathrm{III}\,2\mathrm{s}} + R_{\mathrm{III}} + R_{\mathrm{III}\,1\mathrm{s}} \right)^{-1} \right]^{-1}, \quad (6)$$

where

$$R_{\mathrm{I}} = \left[\left(R_{\mathrm{ct}} \right)^{-1} + \left(R_{\mathrm{I}\,2\mathrm{g}} \right)^{-1} + \left(R_{\mathrm{I\,rd}}{}^{-1} \right) \right]^{-1}, \quad (7)$$

$$R_{\mathrm{II}} = \left[\left(R_{\mathrm{II\,g}} \right)^{-1} + \left(R_{\mathrm{II\,rd}} \right)^{-1} \right]^{-1}, \quad (8)$$

$$R_{\mathrm{III}} = \left[\left(R_{\mathrm{ct}} \right)^{-1} + \left(R_{\mathrm{III}\,2\mathrm{g}} \right)^{-1} + \left(R_{\mathrm{II\,rd}} \right)^{-1} \right]^{-1}, \quad (9)$$

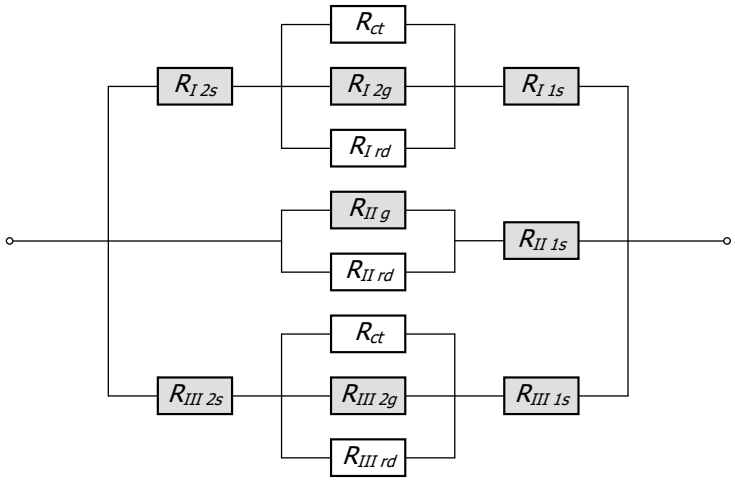

Figure 3. The equivalent system of the individual resistances used to calculate total thermal resistance of the elementary cell R_{ot}.

The method of determining the thermal conduction resistances for all elements in the cell (these resistances in Figure 3 are shown in gray) is described in detail in [17]. When calculating these resistances, one should take into account that the bar thermal conductivity k_{s} and the gas thermal conductivity k_{g} vary with temperature change. In the case analyzed, it was assumed that the material of the bars is low-carbon steel S 235JRH with a maximum carbon content of 0.2% [18], whereas the gas phase is ambient air. Thermal conductivity k_{s} of the assumed grade of steel and thermal conductivity of air are identified with Equations (10) and (11) [19]:

$$k_{\mathrm{s}} = 1.2{\cdot}10^{-8} t^3 - 3.2{\cdot}10^{-5} t^2 - 1.2{\cdot}10^{-2}\, t + 51.3 \quad (10)$$

$$k_{\mathrm{g}} = -2.88{\cdot}10^{-8} t^2 + 8.05{\cdot}10^{-5}\, t + 0.024 \quad (11)$$

The k_{s} and k_{g} coefficients were calculated according to Equations (10) and (11) for the temperatures selected and are presented in Table 1.

Table 1. The k_s and k_g coefficients for selected temperatures.

Temperature, °C	k_s, W/(m K)	k_g, W/(m K)
25	51.0	0.026
200	47.7	0.039
400	42.1	0.052
600	35.2	0.062
800	27.4	0.071

The thermal contact resistance R_{ct} between adjacent bars is calculated from an empirical equation (Equation (12)) [20]:

$$R_{ct} = \left(C_1 t^2 + C_2 t + C_3\right) \cdot 10^{-4} \tag{12}$$

where

$$C_1 = 0.0023 d_p + 5 \cdot 10^{-5} \tag{13}$$

$$C_2 = -1.96 d_p - 0.036 \tag{14}$$

$$C_3 = 1346.5 d_p + 47.8 \tag{15}$$

In the case of thermal radiation, the resistance R_{rd} for the entire cell is calculated with Equation (16). The space of radiation heat transfer in this system is enclosed by four surfaces: A_1, A_I, A_{gp}, and A_{III}. The thermal resistance for radiation R_{rd} in this system is calculated from the radiosity balance method [16,21]. After rearranging, the equation for this resistance is in the form given in Equation (16) [14]:

$$R_{rd} = \frac{X_{rd}}{4\sigma T^3} \tag{16}$$

where X_{rd} is a dimensionless coefficient with its value depending on the bar emissivity ε and its shape, together with the relative position of the surfaces that closed the space of radiation exchange; T is the absolute mean temperature of all surfaces. For the arrangement of the surfaces in the cell considered, coefficient X_{rd} is described by Equation (17) [22]:

$$X_{rd} = \frac{2l_p + l_{ga}}{\left(1.59 d_p - 2A_I\right)\left(\frac{1}{\varepsilon} + \frac{A_I}{2A_I + A_{gp}}\left(\frac{1}{\varepsilon} - 1\right)\right)^{-1}}, \tag{17}$$

Radiation resistances $R_{I\,rd}$, $R_{II\,rd}$, and $R_{III\,rd}$ related to the individual sections are described by Equations (18) and (19):

$$R_{I\,rd} = R_{III\,rd} = \frac{l_p}{2l_p + l_{gp}} \frac{X_{rd}}{4\sigma T^3} \tag{18}$$

$$R_{II\,rd} = \frac{l_{gp}}{2l_p + l_{gp}} \frac{X_{rd}}{4\sigma T^3} \tag{19}$$

The effective thermal conductivity k_{ef} of the cell is defined by the equation of thermal conduction resistance in the flat, homogeneous layer (Equation (20)) [16]:

$$k_{ef} = \frac{\delta_K}{R_{to}}, \tag{20}$$

In turn, the k_{es} coefficient is calculated under the assumption that there is no radiation heat transfer within the cell (Equation (21)). Adjusted total thermal resistance $R_{to\,a}$, used in

this case, is calculated according to Equation (22). The equivalent electric analog system of the thermal resistances, taken for consideration in this case, is shown in Figure 4.

$$k_{es} = \frac{\delta_K}{R_{to\ a}}, \tag{21}$$

where

$$R_{to\ a} = [(R_{I\ 2s} + R_{I\ a} + R_{I\ 1s})^{-1} + (R_{II\ g} + R_{II\ 1s})^{-1} + (R_{III\ 2s} + R_{III\ a} + R_{III\ 1s})^{-1}]^{-1}, \tag{22}$$

and

$$R_{I\ a} = \left[(R_{ct})^{-1} + (R_{I\ 2g})^{-1}\right]^{-1}, \tag{23}$$

$$R_{III\ a} = \left[(R_{ct})^{-1} + (R_{III\ 2g})^{-1}\right]^{-1}, \tag{24}$$

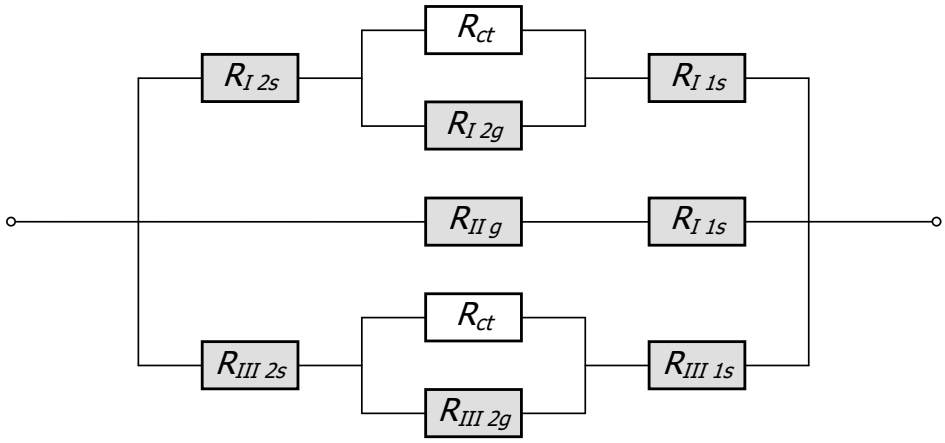

Figure 4. The equivalent electric system of the resistances used to calculate adjusted total thermal resistance of the elementary cell $R_{to\ a}$.

According to this methodology, the calculations of the F_R factor were realized in the following steps: (i) first, the effective thermal conductivity k_{ef} is determined, (ii) next, the essential thermal conductivity k_{es} is calculated, and (iii) last, the radiation exchange factor F_R is calculated from Equation (3).

The calculations included three bar diameters (10, 20, and 30 mm), five emissivity values (0.5, 0.6, 0.7, 0.8, and 0.9), and three bundle porosities. The bundle porosity in the geometric model considered is a function of the gap width l_{gp}. The l_{gp} value is defined as a multiple of the bar diameter; three cases were considered: 0, 0.2 d_p, and 0.4 d_p, which correspond to the following porosities: 0.091, 0.145, and 0.214. The calculations were performed in the temperature range 200 to 800 °C.

3. Results and Discussion

First, the values of the essential thermal conductivity k_{es} were presented (Figure 5) in order to analyze the results of the calculations. These results refer to two bar diameters (10 and 30 mm) and all porosities considered. In the chart (Figure 5), the reference table refers to the bar diameter and porosities used. As can be seen, the k_{es} coefficient increases with increase in the bar diameter and decreases with increase in bundle porosity. In any case, the maximum value occurs at approximately 400 °C. The values obtained for all cases are in the range 1.4 to 3.9 W/(m·K).

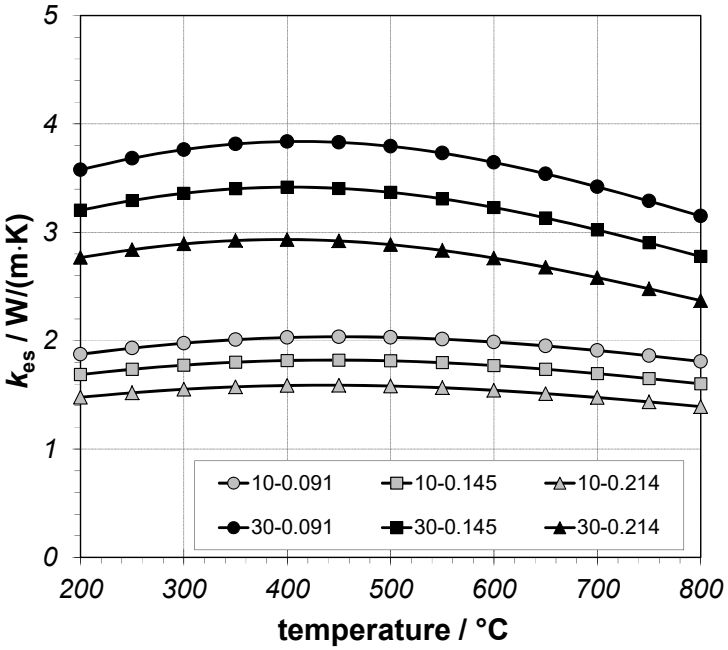

Figure 5. Essential thermal conductivity of 10 and 30 mm bar bundles for three different porosities.

The increase in k_{es} with increase of the bar diameter is caused by the changes in thermal contact resistance R_{ct}. According to Equations (12)–(15), the resistance R_{ct} decreases with increasing bar diameter, which was determined from experimental studies on bars bed samples [19]. In these tests, samples were made of bars with diameters of 10, 20, 30, and 40 mm. It is well known that thermal contact resistance depends on the contact area between the adjacent elements [23,24]. For adjacent bars, the contact area is greater when the bars are straighter. It was found that the smaller the diameter of the bars, the less straight they are, and thus, the samples have a smaller contact area and finally, the resistance R_{ct} increases.

The decrease of the k_{es} coefficient with increase of cavity is caused by heat transfer between successive layers of bars. Heat is transferred here by conduction in the air cavity and contact conduction. When the cavity width is changed, the contact surface between the bars does not change significantly; hence, the contact conduction does not change either. However, increase in the cavity increases the area of conduction in air. This mechanism of heat transfer is much less efficient than contact conduction. As a result, a decrease in contact conduction is observed in relation to overall conduction in air, which contributes to a decrease in the value of k_{es}.

The last question: why is there a maximum of k_{es} at 400 °C? The change in thermal contact resistance R_{ct} is responsible for this change, which is described by Equation (12), obtained from extensive experimental research. The minimum of this resistance appears at temperature of approximately 400 °C. This is due to a number of bar properties that determine the intensity of contact conduction, which include thermal conductivity, Young's modulus E, Poisson's ratio ν, and the surface microhardness H_c. These factors depend on temperature and are mutually connected. For this reason, at the present stage of research, it is difficult to clearly explain how individual factors affect the changes in R_{ct} and thus also on k_{es} as a function of temperature.

Figure 6 shows the radiation thermal conductivity k_{rd}. These results relate to a bundle with a porosity of 0.091, two bar diameters (10 and 30 mm), and three emissivities (0.5, 0.7, and 0.9). It is clearly visible that the coefficient k_{rd} increases with the temperature, emissivity, and bar diameter; the maximum values for all cases are in the range 0.7 to 4.4 W/(m·K).

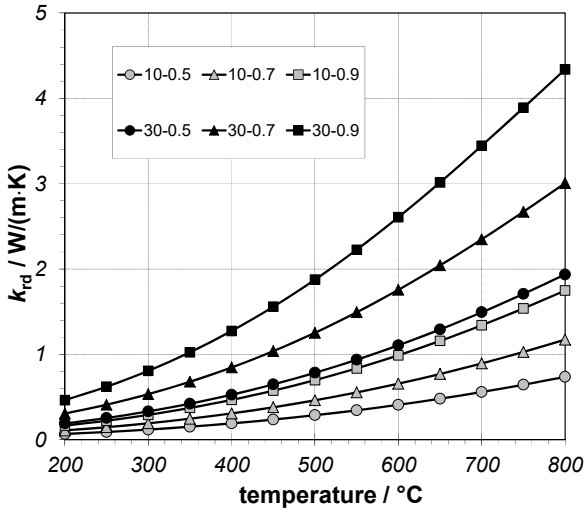

Figure 6. Radiation thermal conductivity of 10 and 30 mm bar bundles with porosity of 0.091.

The next two figures show the changes in the radiation exchange factor F_R as a function of temperature. Figure 7 relates to a 10 mm bar bundle and Figure 8 to a 30 mm bar bundle. As can be seen in all cases, the F_R decreases slightly as a function of temperature, and the amount of this decrease depends on the diameter of the bars. The same effect is observed for the bundle porosity, while F_R increases significantly with the bar emissivity. The F_R values, depending on temperature, bar diameter, bar emissivity, and bundle porosity, are presented in Table 2.

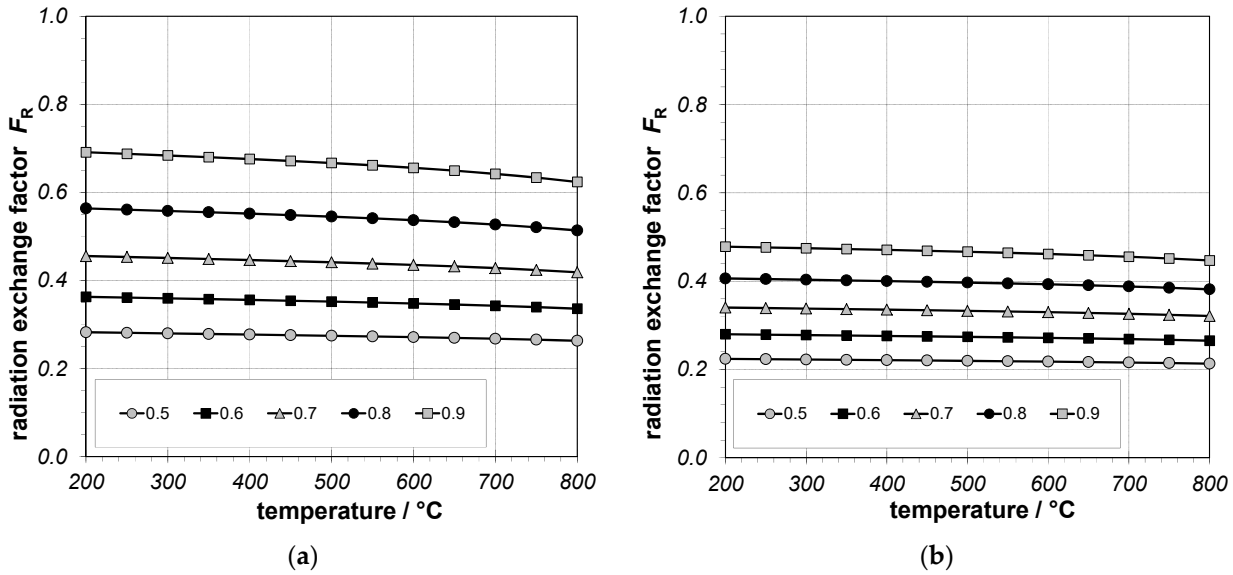

Figure 7. Radiation exchange factor F_R of 10 mm bar bundle: (**a**) result for φ = 0.091 and (**b**) result for φ = 0.214.

Table 2. The F_R values depending on the bar diameter, bar emissivity, and bundle porosity.

Bar Diameter	Bundle Porosity	F_R
10 mm	0.091	0.26 ÷ 0.69
10 mm	0.214	0.21 ÷ 0.48
30 mm	0.091	0.23 ÷ 0.64
30 mm	0.214	0.19 ÷ 0.45

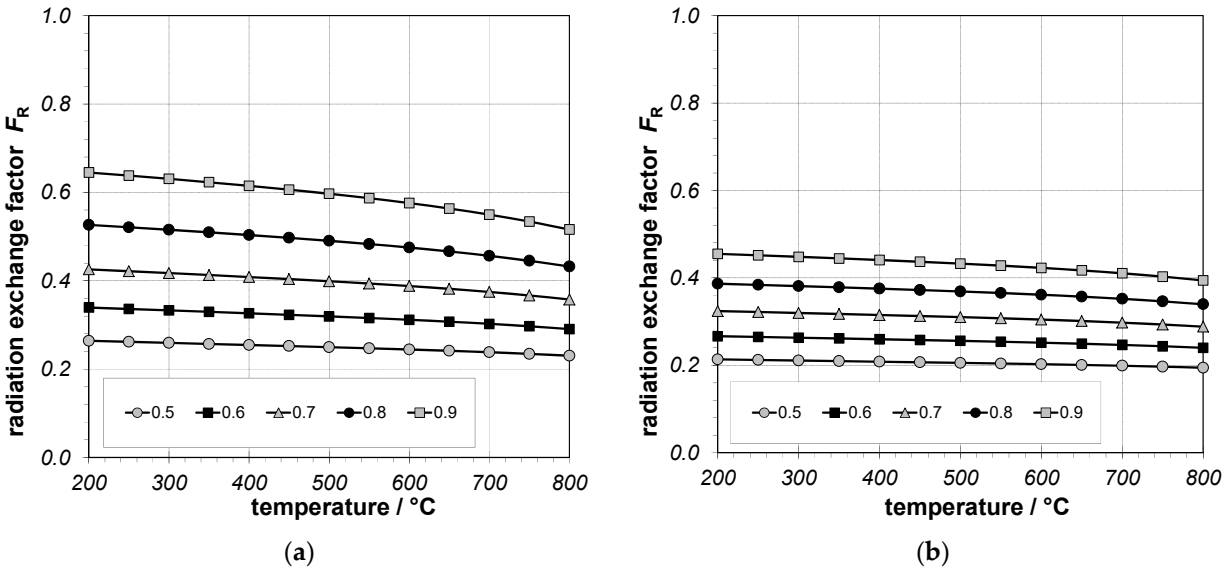

Figure 8. Radiation exchange factor F_R of 30 mm bar bundle: (**a**) result for φ = 0.091 and (**b**) result for φ = 0.214.

In the next stage of the analysis, radiation exchange factors averaged for the entire temperature range were estimated for each computational case. The F_R values obtained in this way, depending on emissivity and bar diameter, are shown in Figure 9. Figure 9a relates to the bundle with a porosity of 0.091, while Figure 9b relates to the bundle with porosity of 0.214. Note that regardless of porosity, radiation exchange factor depends slightly on the bar diameter. Therefore, it was required to reaverage F_R taking into account the bar diameter. The final averaged F_R values obtained in this way, both as a function of bar emissivity and the bundle porosity, are shown in Figure 10. As referenced, parameter F_R for all porosities changes almost linearly as a function of the bar emissivity. Therefore, in order to generalize the results obtained, regression functions were determined using Equation (25):

$$F_R = B_1\varepsilon + B_2, \tag{25}$$

The B_1 and B_2 coefficients from Equation (25) corresponding to the individual bundle porosities are presented in Table 3.

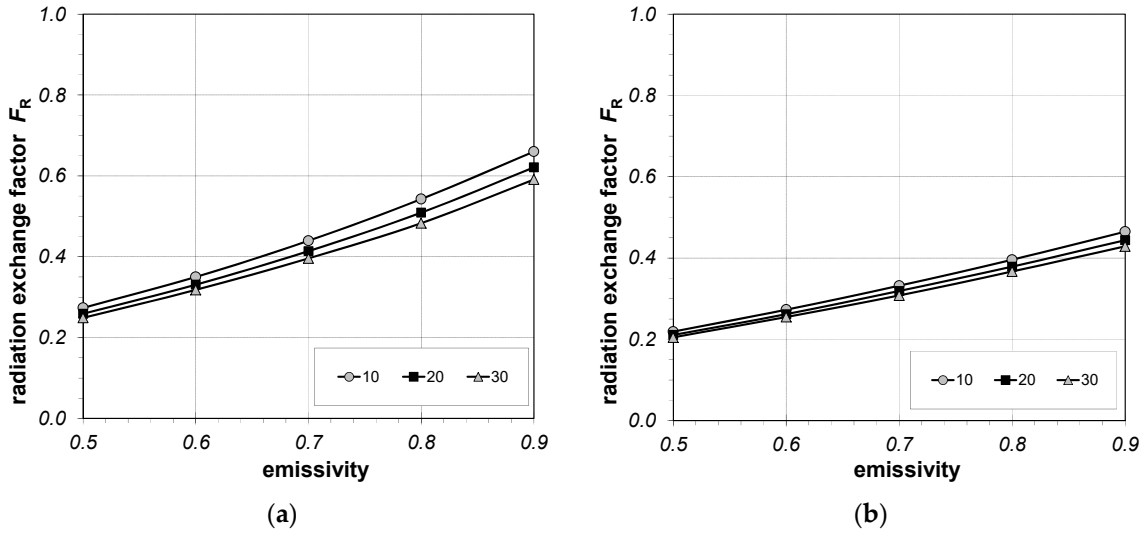

Figure 9. Temperature-averaged F_R: (**a**) result for φ = 0.091 and (**b**) result for φ = 0.214.

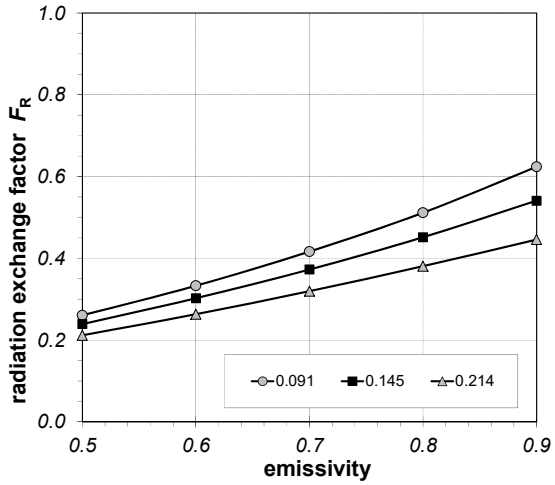

Figure 10. Final averaged F_R for different emissivity and porosity.

Table 3. The B_1 and B_2 coefficients from Equation (25) corresponding to the individual bundle porosities.

Bundle Porosity	B_1	B_2
0.091	0.905	–0.205
0.145	0.753	–0.146
0.214	0.586	–0.086

As established, both B_1 and B_2 change almost linearly as a function of the bundle porosity φ, which can be described by Equations (26) and (27):

$$B_1 = -2.586\ \varphi + 1.136, \tag{26}$$

$$B_2 = 0.963\ \varphi - 0.29 \tag{27}$$

Based on Equations (25)–(27), it is possible to present a generalized relationship describing changes in F_R parameter both as a function of the bar emissivity and bundle porosity (Equation (28)):

$$F_R = (-2.586\ \varphi + 1.136)\varepsilon + 0.963\ \varphi - 0.29, \tag{28}$$

Based on Equation (28), it is possible to formulate one simple algebraic relationship to determine the radiation thermal conductivity k_{rd} of the bar bundle (Equation 29):

$$k_{rd} = 4[((-2.586\ \varphi + 1.136)\varepsilon + 0.963\ \varphi - 0.29)]\sigma d_p T^3, \tag{29}$$

As a result of the Equation (29), some simplifications have been made concerning averaging over the bar diameters and temperatures. Therefore, the value of the coefficient k_{rd} calculated using this relationship is characterized by a certain inaccuracy. This inaccuracy can be described by the relative percentage discrepancy (RPD) with Equation (30):

$$\mathrm{RPD} = \frac{k_{rd\text{-}ex} - k_{rd\text{-}sp}}{k_{rd\text{-}ex}} \cdot 100\%, \tag{30}$$

where $k_{rd\text{-}ex}$ is obtained from the thermal resistance's analysis (exact approach) and $k_{rd\text{-}sp}$ is calculated with Equation (29).

Figure 11 shows the results of the RPD parameter depending on the temperature and porosity for a 30 mm bar bundle and 0.8 emissivity. As can be seen, the largest changes in RPD were recorded for the lowest porosity. In this case, the analyzed parameter changed with the temperature increases from 6% to −9%. From the industrial practice point of view, the inaccuracy of calculations of the radiation thermal conductivity at this level

is acceptable. Importantly, after averaging over the entire temperature range, the RPD value was only 0.2%. Thus, Equation (19) can be used to determine the radiative thermal conductivity as one of the basic thermal properties of the bar bundle.

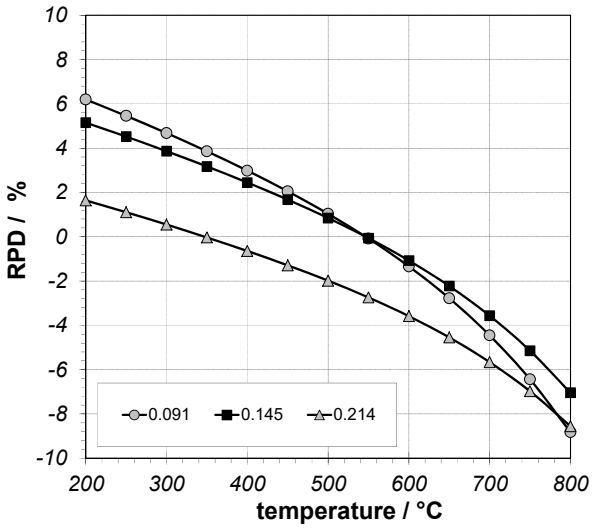

Figure 11. The RPD parameter depending on temperature and porosity for 30 mm bar bundle and 0.8 emissivity.

4. Conclusions

The article presents an innovative methodology for determining the radiation exchange factor for steel bar bundles. The analysis performed resulted in formulation of a new equation that determines the parameter F_R correlated with the emissivity of the bars and the porosity of a bundle. Results show that the F_R depends on the bar diameter, emissivity, and bundle porosity, and it is in the range 0.19 to 0.69. The main advantage of this methodology is its simplicity; hence, potential errors can be quickly identified and removed. It also allows calculations of the k_{rd} coefficient. Other methods for determining these parameters are based on the analysis of thermal resistance and require several sophisticated numerical calculations. It needs to be highlighted that Equation (28) is limited in terms of the material porosity. The maximum porosity of the bundle for which the equation can be used is 0.22. This limitation applies to the geometry of the elementary cell, which was used to analyze the thermal resistance in the medium considered.

The radiation heat transfer for surface to surface condition can be solved with the aid of CFD analysis. However, in order to perform such research, one must have appropriate commercial CFD software. In contrast, building our own code for CFD solution requires high skills in both programming (usually in C, C+), mesh generating, and solving partial differential equations. Additionally, the CFD techniques also require specialist knowledge and skills, which are laborious and time-consuming (long calculation times). Conversely, the model presented by the authors in the form of one simple algebraic equation allows for fast and reliable calculations as these calculations are based on simple correlations. Summarizing, the simple method proposed, which does not require CFD analysis, provides reliable results; hence, this is the main innovation of this study.

Author Contributions: Conceptualization, R.W. and M.G.; methodology, R.W. and M.G.; software, S.S. and A.P.; measurements, R.W.; validation, S.S. and R.W.; formal analysis, R.W., S.S. and A.P.; writing—original draft preparation, R.W., A.P. and M.G.; visualization, S.S.; supervision, M.G. All authors have read and agreed to the published version of the manuscript.

Funding: This research received no external funding.

Institutional Review Board Statement: Not applicable.

Informed Consent Statement: Not applicable.

Data Availability Statement: Not applicable.

Conflicts of Interest: The authors declare no conflict of interest.

References

1. Musiał, M. Numerical Analysis of the Process of Heating of a Bed of Steel Bars. *Arch. Metall. Mater.* **2013**, *1*, 63–66. [CrossRef]
2. Sahay, S.S.; Krishnan, K. Model Based Optimization of Continuous Annealing Operation for Bundle of Packed Rods. *Ironmak. Steelmak.* **2007**, *29*, 89–94. [CrossRef]
3. Sahay, S.; Mehta, R.; Krishnan, K. Genetic-Algorithm-Based Optimization of an Industrial Age-Hardening Operation for Packed Bundles of Aluminum Rods. *Mater. Manuf. Process.* **2007**, *22*, 615–622. [CrossRef]
4. Sahay, S.S.; Krishnan, K.; Kuthle, M.; Chodha, A.; Bhattacharya, A.; Das, A.K. Model-Based Optimization of a Highly Automated Industrial Batch Annealing Operation. *Ironmak. Steelmak.* **2006**, *33*, 306–314. [CrossRef]
5. Kaviany, M. *Principles of Heat Transfer in Porous Media*, 2nd ed.; Springer: New York, NY, USA, 1995; pp. 119–131.
6. Kwon, J.S.; Jang, C.H.; Jung, H.; Song, T.H. Effective Thermal Conductivity of Various Filling Materials for Vacuum Insulation Panels. *Int. J. Heat Mass Transf.* **2009**, *52*, 5525–5532. [CrossRef]
7. Wei, G.; Zhang, X.; Yu, F. Effective Thermal Conductivity Analysis of Xonotlite–Aerogel Composite Insulation Material. *J. Therm. Sci.* **2009**, *18*, 142–149. [CrossRef]
8. Van Antwerpen, W.; du Toit, C.G.; Rousseau, P.G.A. Review of Correlations to Model the Packing Structure and Effective Thermal Conductivity in Packed Beds of Mono-Sized Spherical Particles. *Nucl. Eng. Des.* **2010**, *240*, 1803–1818. [CrossRef]
9. Kaviany, M.; Singh, B.P. Radiative Heat Transfer in Packed Beds. In *Heat and Mass Transfer in Porous Media*; Quintard, M., Todorovic, M., Eds.; Elsevier: Amsterdam, The Netherlands, 1992; pp. 191–202.
10. Cheng, J.C.; Churchill, S.W. Radiant Transfer in Packed Beds. *AIChE J.* **1963**, *9*, 35–41. [CrossRef]
11. Vortmeyer, D. Radiation in Packed Solids. In *Heat Transfer 1978 Proceedings of the Sixth International Heat Transfer Conference*; Rogers, J.R., Ed.; Hemisphere: Washington, DC, USA, 1978; pp. 525–539.
12. Wakao, N.; Wato, K. Effective Thermal Conductivity of Packed Beds. *J. Chem. Eng.* **1968**, *2*, 24–33. [CrossRef]
13. Argo, W.B.; Smith, J. Heat Transfer in Packed Beds. *Chem. Eng. Prog.* **1996**, *49*, 443–451.
14. Wyczólkowski, R.; Urbaniak, D. Modeling of Radiation in Bar Bundles Using the Thermal Resistance Concept. *J. Thermophys. Heat Transf.* **2016**, *30*, 721–729. [CrossRef]
15. Kasparek, G.; Vortmeyer, D. Wärmestachlung in Schütungen aus Kuglen mit Vernachlässigbaren Wärmeleitwiderstand. *Wärme und Stoffübertragung* **1976**, *9*, 117–128. (In German) [CrossRef]
16. Cengel, Y.A. Chapter 3. Steady Heat Conduction. In *Heat Transfer and Mass Transfer—A Practical Approach*, 3rd ed.; McGraw–Hill: New York, NY, USA, 2002; pp. 131–149.
17. Wyczolkowski, R.; Gała, M.; Boryca, J. Computational Model of Heat Conduction in the Steel Round Bar Bundle. *Acta Phys. Pol. A* **2019**, *135*, 1001–1007. [CrossRef]
18. European Steel and Alloy Grades/Numbers Steel Number. Available online: http://www.steelnumber.com/en/steel_composition_eu.php?name_id=645 (accessed on 30 July 2021).
19. Wyczółkowski, R. Computational model of complex heat flow in the area of steel rectangular section. *Procedia Eng.* **2016**, *157*, 185–192. [CrossRef]
20. Wyczolkowski, R. *Modelling of Effective Thermal Conductivity of the Steel Porous Charge Using the Thermal Resistance Concept*; Series Monographs 67; Czestochowa University of Technology: Czestochowa, Poland, 2017; pp. 93–98. (In Polish)
21. Modest, M.F. Chapter 5. Radiative Exchange between Gray, Diffuse Surfaces. In *Radiative Heat Transfer*, 3rd ed.; Academic Press: New York, NY, USA; San Francisco, CA, USA; London, UK, 2013; pp. 160–198.
22. Wyczółkowski, R.; Boryca, J. Analysis of Thermal Radiation in the Heating of Steel Round Bar Bundles. *Acta Phys. Pol. A* **2019**, *135*, 256–262. [CrossRef]
23. Furmański, P.; Wiśniewski, T.S.; Banaszek, J. *Thermal Contact Resistances and Other Thermal Phenomena at Solid-Solid Interface*; Institute of Heat Engineering—Warsaw University of Technology: Warsaw, Poland, 2008.
24. Mikic, B.B. Thermal contact conductance: Theoretical consideration. *Int. J. Heat Transf.* **1974**, *17*, 205–214. [CrossRef]